Springer

KSME

Journal of Mechanical Science and Technology 33 (9) (2019) 4081~4091
www.springerlink.com/content/1738-494x(Print)/1976-3824(Online)
DOI 10.1007/s12206-019-0803-2

Frequency-domain approach for the parametric identification of structures with modal interference [†]

Chang-Sheng Lin[*]

Department of Vehicle Engineering, National Pingtung University of Science and Technology, Pingtung, Taiwan

(Manuscript Received October 7, 2018; Revised February 24, 2019; Accepted May 23, 2019)

Abstract

This study aims to improve the accuracy of the parametric estimation of systems with modal interference in the frequency domain. The theory of modal identification states that the frequency response function can be expressed as a rational function form by using the curve fitting technique, and the modal parameters can then be estimated from rational fractional coefficients. The conventional common denominator model only indicates the frequency response function of a single-degree-of-freedom system; thus, it cannot acquire the mode shape information. In this paper, we propose the matrix-fractional coefficient model constructed by the frequency response functions of a multiple-degree-of-freedom system for modal identification. To avoid the phenomenon of omitted modes caused by the distortion from modal interference among the vibration modes of systems during modal estimation, we use a system model with higher-order matrix-fractional coefficients, but fictitious modes may be caused by numerical computation. Structural and fictitious modes can be effectively separated by using a different-order constructed stabilization diagram. Modal identification can be implemented by solving the eigenproblem of the companion matrix yielded from least-square estimation. Numerical simulations, including a full model of sedan and one-half railway vehicle in the form of a linear 2D model, as well as the experimental testing of an actual plate, confirm the validity and robustness of the proposed parametric-estimation method for a system with modal interference under noisy conditions.

Keywords: Parametric identification; Modal interference; Frequency response function; Matrix fraction; Stabilization diagram

1. Introduction

In the system identification of structures, the physical parameter of the stiffness matrix may not be identifiable due to the practical limitation on the number of measurement channels. However, the modal estimation of a linear system is generally implemented from input and output data provided that the system (or the model) is controllable and observable. During modal identification, the content of interference among structural modes often affects the accuracy of modal estimation [1, 2]. Modal interference caused by the close frequency and high damping ratio means that the vibration energy of each mode of the system may overlap with other modes in a certain frequency range. The serious problems of modal interference may lead to difficulties in modal estimation, especially for identifying damping ratios. Accordingly, effective techniques for modal identification must be developed under the distortion from severe modal interference among the vibration modes of systems.

In the past, among many modal estimation techniques, the frequency-domain methods deal with the frequency response functions of a structure under consideration from which modal parameters are estimated. These methods have been used extensively because the frequency response functions are readily available from input and output data [3]. Once the frequency response functions have been obtained, we can implement the modal estimation of a structural system. Fast Fourier transform has been extensively applied to the vibration testing of structures [4]; then, modal estimation in the frequency domain can be developed through frequency response function and spectrum analysis. Spitznogle and Quazi [5] proposed a complex exponential algorithm from the time-limited output data only. In 1981, by using a squared output matrix $\left[h(t)\right]$ consisting of multichannel impulse response functions [6], the least-square complex exponential (LSCE) algorithm was proposed to yield the global estimation of residues and poles. A poly-reference version of the LSCE method, that is, poly-reference complex exponential (PRCE) method [7], was subsequently proposed to implement modal estimation when one of the modes may not be present in structural vibration data. The closely spaced modes (even repeated modes with the same eigenvalues) are resolved using the PRCE method, but the determination of the proper

[*]Corresponding author. Tel.: +886 8 7703202 ext.7454, Fax.: +886 8 7740398
E-mail address: changsheng@mail.npust.edu.tw
[†]Recommended by Associate Editor Junhong Park

model order and modal properties remains subjective through the construction of the stabilization diagram. Richardson and Formenti [8] accomplished a parametric identification from frequency response measurements in the form of rational fraction polynomials by using $\Omega_k = (j\omega)^k$ as a basis function in conjunction with an orthogonal polynomial function. This function may produce ill-conditioned problems in system identification when using the excessive order of basis function $\Omega_k = (j\omega)^k$. Selecting the orthogonal polynomial function in parametric estimation can not only reduce the ill-conditioned problems but also increase relatively many calculations. In 2001, Auweraer et al. [9] proposed a fast-stabilizing parametric estimation method in the frequency domain (LSCF) by using the frequency response function matrix $\left[H(\omega)\right]$ through the curve-fitting technique. In 2003, Guillanume et al. [10] introduced the concept of matrix fraction description to extend LSCF for a poly-reference case and proposed the poly-reference least-square complex frequency-domain (PolyMAX) method. The main advantages of the PolyMAX method are its computation speed and clear stabilization diagrams [11] even with highly noise-contaminated measurement data. However, this method may yield poor estimates in damping ratios especially for a system with heavy damping and insufficient modes to be completely excited under noisy conditions. In addition, by using the stabilization diagram in conjunction with the PolyMAX method, the accuracy of the identification results of structural modes is relatively consistent due to the sufficient order of the model to be estimated; therefore, the system and fictitious modes can be effectively separated [12]. In recent years, the application of the PolyMAX method for modal estimation has been extensively considered [13] and investigated [14]. This method has been adopted for experimental modal analysis and parametric estimation in flight testing of large-scale flutter analysis [15] and can effectively identify the damping ratios of offshore wind turbine on a monopole foundation [16] and estimate the modal parameters of transformer coils [17] in the electric power system. Furthermore, the PolyMAX method has been extended to estimate parameters of a localized frame and implement the damage detection and assessment of large-scale structures [18].

In this paper, we propose the matrix-fractional coefficient model constructed by the frequency response functions of a multiple-degree-of-freedom (MDOF) system to perform the parametric estimation of structures with modal interference. By introducing a higher-order system model in conjunction with the different-order constructed stabilization diagram during modal estimation, identification results are sorted as either structural or fictitious parameters caused by numerical computation. Thus, we can further determine the number of structural modes to be identified. Additionally, the modal parameters of a system, including natural frequencies, damping ratios, and mode shapes, can be obtained by directly solving the eigenproblem of the companion matrix yielded from least-square estimation.

2. Poly-reference least-square complex frequency-domain method

The theory of structural dynamics indicates that the frequency response function can be expressed as a rational function form. Through the curve fitting technique, the response data can be expressed in rational fraction form, and the modal parameters can be obtained from rational fractional coefficients. The conventional frequency-domain method using the common denominator model only indicates the single-degree-of-freedom (SDOF) frequency response function; thus, it cannot acquire the complete modal information. In this study, we use the matrix-fractional coefficients model constructed by MDOF frequency response functions and introduce this model in the estimation procedures of the PolyMAX method for the system identification of structures with modal interference.

The PolyMAX method [10] is based on a frequency response function matrix $\left[H(\omega)\right]$ with symmetric form as primary data containing the FRFs between all inputs and outputs. The coefficients of numerator and denominator matrix polynomials can be identified through the least-square estimation between $\left[H(\omega)\right]$ and the matrix rational mathematical model. The modal parameters of a system can then be estimated from the coefficients of denominator matrix polynomials. The higher the constructed order mathematical model, the more complete the modal information that can be obtained. The sensitivity of polynomial coefficients is, however, affected by high-order polynomial curve fitting. A mathematical model of the frequency response function matrix $\left[H(\omega)\right]$ is a right matrix-fraction model as $\left[H(\omega)\right]=\left[B(\omega)\right]\left[A(\omega)\right]^{-1}$, where $\left[A(\omega)\right]$ and $\left[B(\omega)\right]$ are the common denominator and numerator polynomials between the output and input degrees of freedom (DOFs). Any row in the frequency response function matrix $\left[H(\omega)\right]$ can be expressed as follows:

$$\underline{H}_j(\omega) = \underline{B}_j(\omega)\left[A(\omega)\right]^{-1}, \tag{1}$$

where $j = 1, 2 \cdots n$. The denominator coefficient polynomial $\left[A(\omega)\right]$ and numerator coefficient polynomial $\underline{B}_j(\omega)$ are respectively defined as

$$\begin{aligned} \underline{B}_j(\omega) &= \sum_{k=0}^{m} \underline{\beta}_{jk}\Omega_k(\omega), \\ \left[A(\omega)\right] &= \sum_{k=0}^{m}\left[\alpha_k\right]\Omega_k(\omega), \end{aligned} \tag{2}$$

where $\Omega_k(\omega) = e^{-i\omega_k T_s}$ and T_s is the sampling period. $\underline{\beta}_{jk}$ and $\left[\alpha_k\right]$ are the unknown polynomial coefficients of the numerator vector and denominator matrix, respectively. The order of the numerator polynomial is, in general, not the same as that of the denominator polynomial. m is the polynomial order of the mathematical model, and $\Omega_k(\omega)$ is the polynomial basic function, i.e., a frequency-domain model is derived from a discrete-time model. $\left[H(\omega)\right]$ can be written for all values of the frequency axis of the FRF data. The unknown polynomial coefficients for the numerator vector and denominator matrix polynomials are then found using the least-square method after linearization. The constructed numerator and denominator matrix polynomial model can be viewed as a function of β_i, α, and arbitrary ω_i. The prediction errors $\underline{\varepsilon}_j\left(\underline{\beta}_j,\alpha,\omega_i\right)$ between the constructed numerator/denominator matrix polynomial model $\underline{B}_j\left(\underline{\beta}_j,\omega_i\right)\left[A\left(\alpha,\omega_i\right)\right]^{-1}$ and frequency response function $\underline{\hat{H}}_j\left(\omega_i\right)$ of a system obtained from practical data are defined as follows:

$$\underline{\varepsilon}_j\left(\underline{\beta}_j,\alpha,\omega_i\right)=\underline{B}_j\left(\underline{\beta}_j,\omega_i\right)\left[A\left(\alpha,\omega_i\right)\right]^{-1}-\underline{\hat{H}}_j\left(\omega_i\right). \quad (3)$$

Directly solving Eq. (3) in the form of simultaneous nonlinear equations may be difficult. To obtain the linearization of Eq. (3), we postmultiply Eq. (3) by $\left[A\left(\alpha,\omega_i\right)\right]$ and redefine the prediction errors $\underline{\varepsilon}_j^{new}(\underline{\beta}_j,\alpha,\omega_i)$ as follows:

$$\underline{\varepsilon}_j^{new}(\underline{\beta}_j,\alpha,\omega_i)=B_j(\underline{\beta}_j,\omega_i)-\underline{\hat{H}}_j(\omega_i)\left[A(\alpha,\omega_i)\right]. \quad (4)$$

The prediction error matrix consisting of the prediction- error vectors associated with all values of ω_i of the frequency axis of the FRF data is constructed as follows:

$$\left[E_j(\underline{\beta}_j,\alpha)\right]=\begin{pmatrix}\underline{\varepsilon}_j^{new}(\underline{\beta}_j,\alpha,\omega_1)\\ \underline{\varepsilon}_j^{new}(\underline{\beta}_j,\alpha,\omega_2)\\ \vdots\\ \underline{\varepsilon}_j^{new}(\underline{\beta}_j,\alpha,\omega_{N_f})\end{pmatrix}=\left(\left[X_j\right]\ \left[Y_j\right]\right)\begin{pmatrix}\left[\underline{\beta}_j\right]\\ \left[\alpha\right]\end{pmatrix}, \quad (5)$$

where

$$\left[X_j\right]=\begin{pmatrix}\left[\Omega_0(\omega_1)\ \cdots\ \Omega_m(\omega_1)\right]\\ \vdots\\ \left[\Omega_0(\omega_{N_f})\ \cdots\ \Omega_m(\omega_{N_f})\right]\end{pmatrix},$$
$$\left[Y_j\right]=\begin{pmatrix}-\left[\Omega_0(\omega_1)\ \cdots\ \Omega_m(\omega_1)\right]\otimes\hat{H}_j(\omega_1)\\ \vdots\\ -\left[\Omega_0(\omega_{N_f})\ \cdots\ \Omega_m(\omega_{N_f})\right]\otimes\hat{H}_j(\omega_{N_f})\end{pmatrix}, \quad (6)$$

where $\otimes$ denotes the Kronecker product, which is an operation on two matrices of arbitrary size resulting in a block matrix. The Kronecker product is a generalization of the outer product from vectors to matrices and produces the matrix of the tensor product with respect to a standard choice of basis function. To obtain the optimum solution of α and β_i through the least-square method, we define the prediction error $\ell^{LS}(\beta,\alpha)$ in least squares as follows:

$$\ell^{LS}(\beta,\alpha)=\sum_{j=1}^{n}tr\left\{\left[E_j(\underline{\beta}_j,\alpha)\right]^H\left[E_j(\underline{\beta}_j,\alpha)\right]\right\}. \quad (7)$$

Given the complex numbers in conjugate pairs by solving the roots of denominator coefficient polynomial $\left[A(\omega)\right]$, we assume that $\underline{\beta}_j$ and $\left[\alpha\right]$ are constrained to real-valued coefficients and matrix. Only the real part in Eq. (7) would be considered, and the prediction error $\ell^{LS}(\beta,\alpha)$ can be expressed as follows:

$$\ell^{LS}(\beta,\alpha)=\mathrm{tr}\left\{\left(\left[\beta\right]^T\ \left[\alpha\right]^T\right)\left[\mathrm{Re}(J^HJ)\right]\begin{pmatrix}\left[\beta\right]\\ \left[\alpha\right]\end{pmatrix}\right\}, \quad (8)$$

where

$$\left[\mathrm{Re}(J^HJ)\right]=\begin{pmatrix}\left[R_1\right] & 0 & \cdots & 0 & \left[S_1\right]\\ 0 & \left[R_2\right] & \cdots & 0 & \left[S_2\right]\\ \vdots & \vdots & \ddots & \vdots & \vdots\\ 0 & 0 & \cdots & \left[R_n\right] & \left[S_n\right]\\ \left[S_1\right]^T & \left[S_2\right]^T & \cdots & \left[S_n\right]^T & \left[\sum_{j=1}^{n}T_j\right]\end{pmatrix}, \quad (9)$$

and

$$\begin{aligned}\left[R_j\right]&=\left[\mathrm{Re}(X_j^HX_j)\right]\\ \left[S_j\right]&=\left[\mathrm{Re}(X_j^HY_j)\right]\\ \left[T_j\right]&=\left[\mathrm{Re}(Y_j^HY_j)\right]\end{aligned}, \quad (10)$$

Then, we will select $\underline{\beta}_j$ and $\left[\alpha\right]$ such that the measure of fit $\ell^{LS}(\beta,\alpha)$ is minimized. $\ell^{LS}(\beta,\alpha)$ is partially differentiated with respect to $\underline{\beta}_j$ and $\left[\alpha\right]$, and the result is equated to zero:

$$\begin{aligned}\frac{\partial\ell^{LS}(\beta,\alpha)}{\partial\underline{\beta}_j}&=2(\left[R_j\right]\underline{\beta}_j+\left[S_j\right]\left[\alpha\right])=0,\\ \frac{\partial\ell^{LS}(\beta,\alpha)}{\partial\left[\alpha\right]}&=2\sum_{j=1}^{n}(\left[S_j\right]^T\underline{\beta}_j+\left[T_j\right]\left[\alpha\right])=0.\end{aligned} \quad (11)$$

The normal equation is obtained from Eq. (11) as follows:

$$\left\{2\sum_{j=1}^{n}(\left[T_j\right]-\left[S_j\right]^T\left[R_j\right]^{-1}\left[S_j\right])\right\}\left[\alpha\right]=0. \quad (12)$$

$\left[T_j\right]$, $\left[S_j\right]$, and $\left[R_j\right]$ can be obtained by substituting Eq. (6) into Eq. (10). To avoid a relatively high polynomial order to be chosen for obtaining numerous zero coefficients of polynomials, we set $\left[\alpha_m\right]=\left[I\right]$, where $\left[\alpha_m\right]$ is the highest polynomial order of the denominator matrix polynomial model.

To simplify the procedure of the PolyMAX method, we directly estimate the modal parameters of a structure by solving the eigenvalue problem associated with the companion matrix constructed by denominator polynomial coefficients. On the basis of the property of companion matrix, modal identification can be implemented by directly solving the eigenproblem of the companion matrix instead of solving the coefficients of the numerator and denominator matrix polynomials in rational function form of $\left[H(\omega)\right]$. This approach significantly reduces the relatively many computations required in the conventional PolyMAX method. After deriving the denominator coefficient, the poles (indicating the information of natural frequencies and damping ratios) and mode shape vectors of a system are directly related to the eigenvalues and eigenvectors of their companion matrix. One can derive the following:

$$\begin{bmatrix} [0] & [I] & \cdots & [0] & [0] \\ [0] & [0] & \cdots & [0] & [0] \\ \vdots & \vdots & \ddots & \vdots & \vdots \\ [0] & [0] & \cdots & [0] & [I] \\ -[\alpha_0]^{\mathrm{T}} & -[\alpha_1]^{\mathrm{T}} & \cdots & -[\alpha_{m-2}]^{\mathrm{T}} & -[\alpha_{m-1}]^{\mathrm{T}} \end{bmatrix} [V] = [V][\Lambda], \tag{13}$$

where $[V] = \left[[I]\underline{\phi} \quad [I]\underline{\phi}e^{j\omega\Delta t} \quad [I]\underline{\phi}e^{j\omega 2\Delta t} \quad \cdots \quad [I]\underline{\phi}e^{j\omega(m-1)\Delta t}\right]^T$ is the eigenvector matrix and $[\Lambda]$ is the eigenvalue matrix consisting of the diagonal element $e^{\lambda_r \Delta t}$. λ_r's are the complex numbers in conjugate pairs and the roots of denominator coefficient polynomial $[A(\omega)]$. The dimension of matrix $[I]$ depends on the order of a system to be identified, which can be estimated from the rich frequency content around the structural modes of interest through the stabilization diagram with a different order or frequency response function of the structural system. λ_r's are related to the natural frequencies ω_r and damping ratios ξ_r of the system as follows:

$$\lambda_r \ , \ \lambda_r^* = -\xi_r \omega_r \pm j\sqrt{1-\xi_r^{\,2}}\,\omega_r \, . \tag{14}$$

The mode shape vectors of a system correspond to the eigenvectors related to the eigenvalues λ_r's.

3. Estimation of identified modes from the phase of frequency response function

In general, by examining the Fourier spectrum associated with each of the response channels, one can estimate the number of structural modes to be identified. However, such approach may lead to a distortion in the quantity estimation of identified modes due to the modal interference among the modes with relatively heavy damping and closely spaced modes. To estimate the natural frequencies and number of structural modes to be identified, the phase of the frequency of response function will be used in modal identification. On the basis of the theory of structural dynamics, the phase φ_H of the frequency of response function $H(\bar{\omega})$ associated with an SDOF system will vary instantaneously from -90° to 90° when natural frequencies of a structure are equal to the applied loading frequency. Hence, we can estimate the number of structural modes to be identified by roughly examining the phase φ_H of the frequency of response function $H(\bar{\omega})$ [19]. However, for most MDOF systems in practice, the number of structural modes to be identified may be erroneously determined due to the distortion in modal-identification information among the modes with relatively heavy damping and closely spaced modes. In the case of the two-DOF system, the corresponding frequency of response function $H(\bar{\omega}_r)$ can be expressed as follows:

$$H(\bar{\omega}_r) = \sum_{r=1}^{2} \frac{1}{K_r}\left[\frac{1-\bar{\omega}_r^2}{(1-\bar{\omega}_r^2)^2+(2\xi_r\bar{\omega}_r)^2} + i\frac{-2\xi_r\bar{\omega}_r}{(1-\bar{\omega}_r^2)^2+(2\xi_r\bar{\omega}_r)^2}\right], \tag{15}$$

where $\bar{\omega}_r$ and ξ_r denote the frequency and damping ratios of the rth mode of a system. The phase θ_H of $H(\bar{\omega}_r)$ can be defined as

$$\theta_H = \tan^{-1}\left(\frac{\left(1-\bar{\omega}_1^2\right)\left(-2\xi_2\bar{\omega}_2\right)+\left(1-\bar{\omega}_2^2\right)\left(-2\xi_1\bar{\omega}_1\right)}{\left(1-\bar{\omega}_1^2\right)\left(1-\bar{\omega}_2^2\right)-\left(2\xi_1\bar{\omega}_1\right)\left(2\xi_2\bar{\omega}_2\right)}\right), \tag{16}$$

where $\bar{\omega}_1 = \omega/\omega_1$ and $\bar{\omega}_2 = \omega/\omega_2$. ω, ω_1, and ω_2 are the applied loading, first natural free-vibration, and second natural free-vibration frequencies, respectively. In Eq. (16), the phase θ_H of the frequency of response function $H(\bar{\omega}_r)$ will vary instantaneously from $-90°$ to $90°$ when either the first or second natural free-vibration frequency of a structure equals the applied loading frequency. If the system has a serious problem with modal interference induced by close (even repeated) mode [i.e., $\omega_1 \approx \omega_2 \approx \omega$], in which $\bar{\omega}_1 \approx \bar{\omega}_2$, or heavy damping [i.e., $\xi_r \geq 10\%$], then we cannot relatively accurately determine the natural frequencies and number of structural modes by examining the phase θ_H of the frequency of response function. This case due to the distortion the modal-identification information among the modes with relatively heavy damping and closely spaced modes. The more serious the problem of modal interference is, the more distortion the information of modal estimation has.

The modal interference among modes will be considerable due to the closely coupled modes and may lead to a curve-fitting problem associated with the frequency response function that involves the estimation of the appropriate model size. All MDOF curve-fitting methods assume that interference exists among all modes. The frequency response function data at any frequency is a summation of contributions from all modes. To avoid the phenomenon of omitted modes during the modal identification of systems with modal interference, we use a higher-order model, but fictitious modes may be caused by numerical computation. The system and fictitious modes can be separated by using the different-order constructed stabilization diagram. This diagram is a powerful tool for effectively estimating the accurate number of poles, i.e., polynomial model order, for the PolyMAX method. The idea behind the stabilization diagram is to repeat the estimation process with a different polynomial model order each time. The stable poles should remain constant for all or most of the iterations, and then the polynomial model order can be determined. By using a stabilization diagram to estimate the stable poles, the curve-fitting problem involved in the modal interference can be solved through different model sizes.

4. Numerical simulations

The modal identification can be performed from the excitation and response data of a structural system under external force excitation in dynamic tests. However, obtaining the exact modal information in the practical dynamic testing of large-scale structure is difficult. Consequently, the effectiveness of the present method must be verified in advance through the numerical simulations. To demonstrate the effectiveness of the proposed method, we consider a six-DOF chain-model system with a pair of closely spaced modes (frequency separation smaller than 0.42 rad/sec) and high damping ratios (whose values are above 10 % except for the first mode). Fig. 1 shows a schematic representation of this model. The mass matrix $\boldsymbol{M}$, stiffness matrix $\boldsymbol{K}$, and damping matrix $\boldsymbol{C}$ of the system are given as follows:

$$\boldsymbol{M} = \begin{bmatrix} 1 & 0 & 0 & 0 & 0 & 0 \\ 0 & 1 & 0 & 0 & 0 & 0 \\ 0 & 0 & 2 & 0 & 0 & 0 \\ 0 & 0 & 0 & 2 & 0 & 0 \\ 0 & 0 & 0 & 0 & 1 & 0 \\ 0 & 0 & 0 & 0 & 0 & 1 \end{bmatrix} \text{kg}$$

$$\boldsymbol{K} = 600 * \begin{bmatrix} 2 & -1 & 0 & 0 & 0 & 0 \\ -1 & 2 & -1 & 0 & 0 & 0 \\ 0 & -1 & 2 & -1 & 0 & 0 \\ 0 & 0 & -1 & 2 & -1 & 0 \\ 0 & 0 & 0 & -1 & 2 & -1 \\ 0 & 0 & 0 & 0 & -1 & 2 \end{bmatrix} \text{N/m}$$

$$\boldsymbol{C} = 0.05\boldsymbol{M} + 0.01\boldsymbol{K} \ \text{N} \cdot \text{sec/m}.$$

The chain-model system has proportional damping, because the damping matrix $\boldsymbol{C}$ can be expressed as a linear combination of $\boldsymbol{M}$ and $\boldsymbol{K}$. The simulated impulse function serves as the excitation input acting on each mass point of the system. The sampling interval is chosen as $\Delta t = 0.01$ s, and the sampling period is $T = N_t \cdot \Delta t = 81.92$ s. Assuming that the system is initially at rest, the displacement responses of the system can be obtained using Newmark's method [20]. To consider the measurement noise in practice, we perform modal identification from the simulated impulse response data contaminated with 5 % white noise.

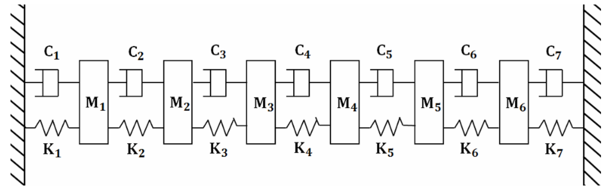

Fig. 1. Schematic plot of the six-DOF chain system.

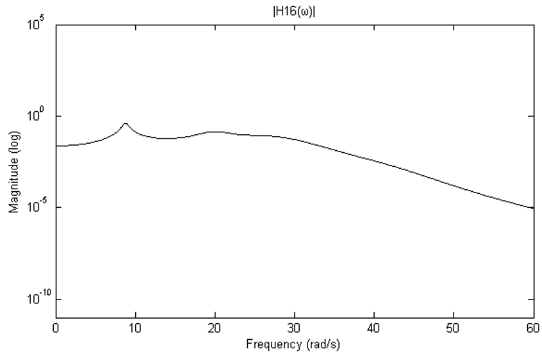

Fig. 2. Typical plot of the amplitude frequency response function $H_{16}(\omega)$ of the system showing modal interference among the structural modes except for the first mode.

To avoid the phenomenon of omitted modes, the polynomial order m in the PolyMAX method must not be less than the number of modes to be identified. However, a continuum structure theoretically has an infinite number of DOFs and modes. By examining the Fourier spectra associated with the measured vibration response histories, the important modes of a system under consideration could not be roughly found because of a distortion in the modal-estimation resulting from a system with modal interference among the vibration modes. Fig. 2 shows the typical plots of the amplitude frequency response functions of the system, wherein the serious problems of modal interference exist in most structural modes except for the first mode. The theory presented in the previous sections indicates that the phase angle diagram of frequency response function, as shown in Fig. 3, cannot be used to determine the number of structural modes influenced by serious modal interference relatively accurately. Thus, the phenomenon of omitted modes from the distortion of system order estimated by frequency response function exists. Only upon the phase angle diagram of frequency response function may lead to an erroneous estimation of the modal frequencies to be identified for the case of a MDOF system with modal interference. A typical plot of the phase frequency response function $H_{16}(\omega)$ shows at least five excited modes of this six-DOF system with modal interference. However, corresponding modal frequencies could not be accurately estimated except the first three structural modes.

Table 1 shows the results of modal estimation when selecting the polynomial order $m = 2$ in the PolyMAX method, indicating that the errors in natural frequencies are less than

Table 1. Results of the modal estimation of a six-DOF chain system with a pair of closely spaced modes and high damping ratios through the PolyMAX method with polynomial order $m = 2$ (contaminated with 5 % white noise).

Mode	Natural frequency (rad/s)			Damping ratio (%)			MAC
	Exact	PolyMAX	Error (%)	Exact	PolyMAX	Error (%)	
1	8.72	8.79	0.81	4.65	5.42	16.65	0.91
2	19.89	19.98	0.45	10.07	11.84	17.57	0.90
3	27.63	27.68	0.17	13.91	16.34	17.50	0.92
4	31.74	31.78	0.13	15.95	18.74	17.50	0.89
5	43.13	43.23	0.23	21.62	25.20	16.54	0.98
6	43.55	43.62	0.15	21.83	25.37	16.19	0.96

Table 2. Results of the modal estimation of a six-DOF chain system with a pair of closely spaced modes and high damping ratios through the PolyMAX method with polynomial order $m = 4$ (contaminated with 5 % white noise).

Mode	Natural frequency (rad/s)			Damping ratio (%)			MAC
	Exact	PolyMAX	Error (%)	Exact	PolyMAX	Error (%)	
1	8.72	8.79	0.81	4.65	4.65	0.08	0.96
2	19.89	19.91	0.10	10.07	10.10	0.09	0.95
3	27.63	27.56	0.26	13.91	13.90	0.05	0.98
4	31.74	31.59	0.47	15.95	15.89	0.37	0.95
5	43.13	43.69	1.29	21.62	21.28	0.59	0.98
6	43.55	43.11	1.02	21.83	21.47	1.67	0.97

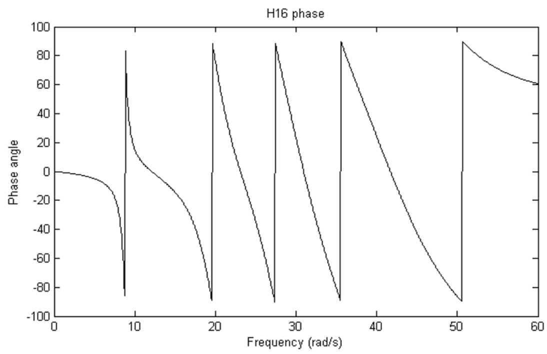

Fig. 3. Typical plot of the phases associated with the frequency response function $H_{16}(\omega)$ of the system with a pair of closely spaced modes and high damping ratios.

1 % and those in damping ratios are around 17 %. The errors of identified damping ratios are higher than those of natural frequencies, which may be due to the system response generally having lower sensitivity to damping ratios. To obtain improved estimation results of damping ratios, we further increase the polynomial order m to reach 4. Table 2 shows the corresponding results of modal estimation when selecting $m = 4$ in the PolyMAX method, indicating that the errors in damping ratios significantly reduce to less than 2 %. The identified mode shapes are compared with the exact values in Fig. 4, in which we observe good agreement with the value of the

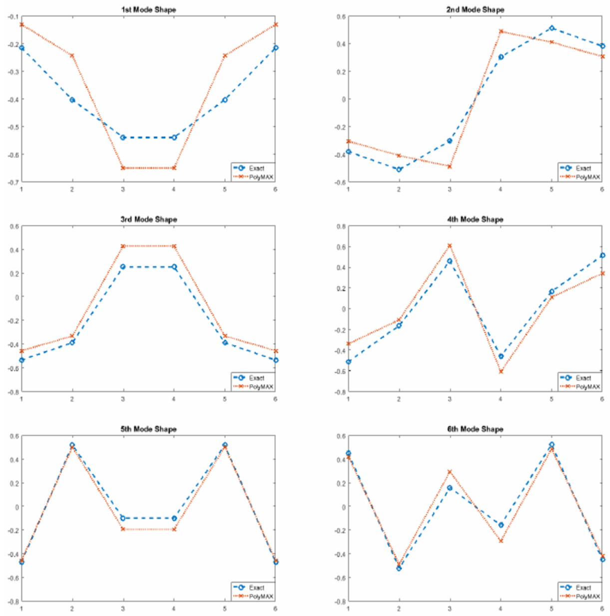

Fig. 4. Comparison between the identified and exact mode shapes of the six-DOF system with a pair of closely spaced modes and high damping ratios.

modal assurance criterion (MAC) [21] of 0.93 on average.

In the proceeding, to avoid the phenomenon of omitted modes during the modal identification of systems with modal interference, we use a higher-order system model through PolyMAX, but fictitious modes may be caused by numerical computation. However, as the correct order of a model to be estimated is often unknown a priori, different model orders are postulated and then the "best" one is selected in accordance with a certain criterion, such as singular value analysis [19] or stabilization diagram method [11]. A stabilization diagram is used to display stable pole groups consisting of natural frequency and damping ratio pairs that exist when applying curve fitting to the data of frequency response function obtained from the measured response histories with different model sizes. This diagram is utilized to determine the number of modes to be identified in structural response data. Extra computational modes are always used with a stabilization diagram to account for the residual effects of additional "out of band modes" in the data and then are ignored in the final modal-estimation results. The system and fictitious modes can be separated by using the constructed stabilization diagram with different-polynomial order, as shown in Fig. 5. The number of structural modes to be identified is six, which is obtained from the stabilization diagram associated with the different polynomial-order $m = 1 \sim 8$. Furthermore, the stabilization diagram shows a relatively evident "location" of natural frequencies of the system, with no clear peak in the amplitude of frequency response function due to the modal interference caused by heavy damping.

To demonstrate the effectiveness of the present method for relatively complicated structural systems, we further consider

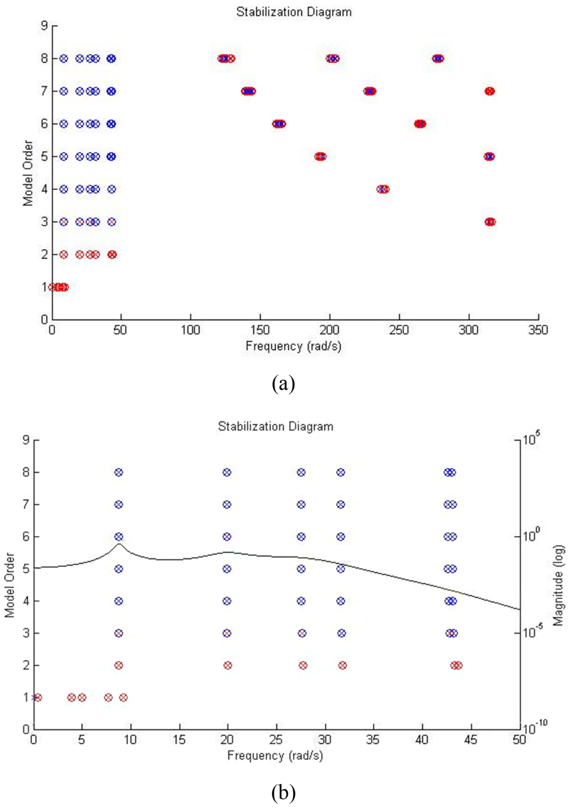

Fig. 5. Typical plot of the stabilization diagram and $\left[H_{16}(\omega)\right]$ of the system with a pair of closely spaced modes and high damping ratios: (a) Overall; (b) part of frequency information.

a full model of motor vehicle [19] with two pairs of closely spaced modes (frequency separation smaller than 0.2 rad/sec), as shown in Fig. 6. A full model of a motor vehicle can be generally viewed as a seven-DOF system, which includes the bounce, pitch, and roll motions for the body of a motor vehicle, and four bounce motions for the wheels. For further complex systems, the Lagrange equation can be used to derive the equation of motion whose advantage is that only displacement and velocity enter into the energy functions and can be written in a slightly simplified form without using free-body diagrams, as well as summing forces and moments; thus, intricate kinematic calculation of acceleration is avoided [22]. A model of the sedan under consideration, in this case, is a seven-DOF system with $\mathbf{u}=\left[u_1,u_2,u_3,u_4,u_5,u_6,u_7\right]$, where $u_2=\varphi$ and $u_3=\theta$ are the rotational displacements of the pitch and roll behavior of the motor vehicle, respectively, and the others are the vertical displacements of the bounce behavior of the motor vehicle and four wheels, as shown in Fig. 6. The mass matrix is diagonal, diag $\mathbf{M}=\left[m_1,m_2,m_3,m_4,m_5,m_6,m_7\right]$, where the sprung mass m_1 represents the corresponding body mass of the motor vehicle to the wheels and the unsprung mass, m_4, m_5, m_6, and m_7, represents the wheel and its associated components. $m_2=I_y$ and $m_3=I_x$ are the pitch and roll moments of inertia of the motor vehicle, respectively. The stiffness matrix can be obtained as

Table 3. Results of the modal estimation of a seven-DOF system of a motor vehicle through the modified PolyMAX method with polynomial order $m=2$.

Mode	Natural frequency (rad/s)			Damping ratio (%)			MAC
	Exact	PolyMAX	Error (%)	Exact	PolyMAX	Error (%)	
1	5.03	5.11	1.49	1.25	1.21	2.56	0.99
2	7.82	7.89	0.92	1.03	1.01	1.64	0.95
3	18.48	18.50	0.13	1.19	1.18	1.11	0.93
4	73.79	70.77	4.09	3.76	3.45	8.20	0.99
5	73.87	70.85	4.10	3.76	3.45	8.22	0.97
6	87.93	82.93	5.68	4.45	3.96	11.10	0.99
7	88.07	83.05	5.70	4.46	3.96	11.14	0.96

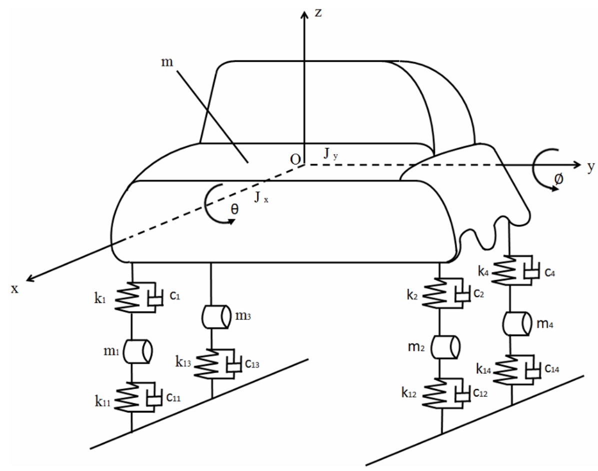

Fig. 6. Schematic plot of the seven-DOF system of a sedan.

$$\mathbf{K}=\begin{bmatrix} k_1+k_2+k_3+k_4 & -L_1k_1+L_2k_2-L_1k_3+L_2k_4 & -L_3k_1-L_3k_2+L_4k_3+L_4k_4 & -k_1 & -k_2 & -k_3 & -k_4 \\ -L_1k_1+L_2k_2-L_1k_3+L_2k_4 & L_1^2k_1+L_2^2k_2+L_1^2k_3+L_2^2k_4 & L_1L_3k_1-L_2L_3k_2-L_1L_4k_3+L_2L_4k_4 & L_1k_1 & -L_2k_2 & L_1k_3 & -L_2k_4 \\ -L_3k_1-L_3k_2+L_4k_3+L_4k_4 & L_1L_3k_1-L_2L_3k_2-L_1L_4k_3+L_2L_4k_4 & L_3^2k_1+L_3^2k_2+L_4^2k_3+L_4^2k_4 & L_3k_1 & L_3k_2 & -L_4k_3 & -L_4k_4 \\ -k_1 & L_1k & L_3k_1 & k_1+k_{11} & 0 & 0 & 0 \\ -k_2 & -L_2k_2 & L_3k_2 & 0 & k_2+k_{12} & 0 & 0 \\ -k_3 & L_1k_3 & -L_4k_3 & 0 & 0 & k_3+k_{13} & 0 \\ -k_4 & -L_2k_4 & -L_4k_4 & 0 & 0 & 0 & k_4+k_{14} \end{bmatrix}$$

where L_1, L_2, L_3, and L_4 are the half of the axle track of the front and rear wheels and the distances to the front and rear axles from the center of gravity of the motor, respectively. The summation of L_3 and L_4 is the wheelbase of a motor. $k_1(=k_2)$, $k_3(=k_4)$, $k_{11}(=k_{12})$, and $k_{13}(=k_{14})$ are the front and rear suspension spring stiffness and the front and rear tire stiffness, respectively. Throughout this numerical study, $\left[m_1,m_4,m_5,m_6,m_7\right]=\left[1365, 46.8, 46.8, 41.4, 41.4\right]$ kg, $m_2=$

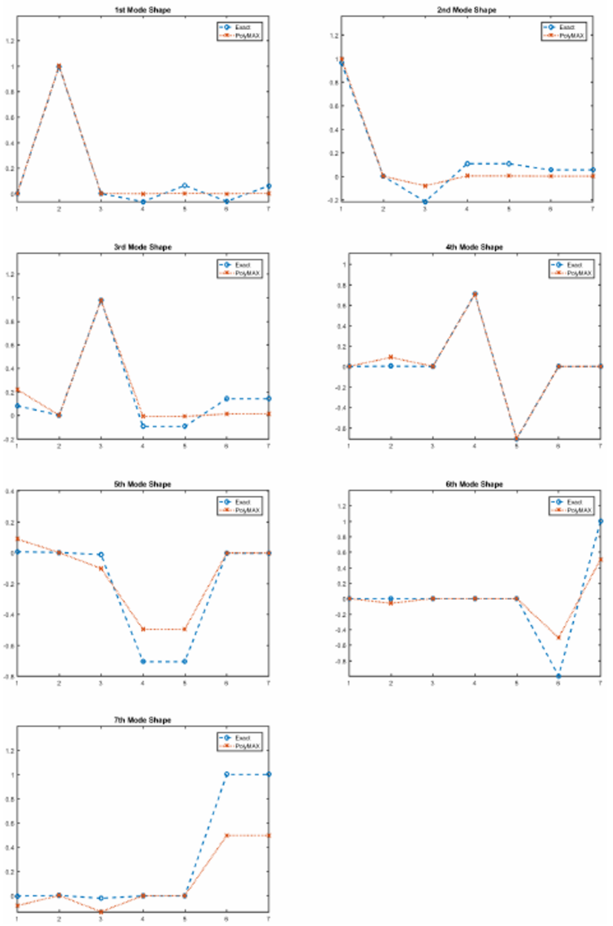

Fig. 7. Comparison between the identified and exact mode shapes of the seven-DOF system of a motor vehicle with two pairs of closely spaced modes.

$I_y = 1.831\times10^3\ \text{kg}\cdot\text{m}^2$, and $m_3 = I_x = 4.98\times10^2\ \text{kg}\cdot\text{m}^2$; $k_1 = k_2 = 2.2428\times10^4$ N/m, $k_3 = k_4 = 2.7022\times10^4$ N/m, $k_{11} = k_{12} = 2.32342\times10^5$ N/m, and $k_{13} = k_{14} = 2.92982\times10^5$ N/m; $L_1 = L_2 = 0.7165$ m, $L_3 = 1.1135$ m, and $L_4 = 1.5415$ m; $\boldsymbol{C} = 0.1\boldsymbol{M} + 0.001\boldsymbol{K}$ N·sec/m. The system of a motor vehicle has proportional damping because the damping matrix $\boldsymbol{C}$ can be expressed as a linear combination of $\boldsymbol{M}$ and $\boldsymbol{K}$. Table 3 summarizes the modal-estimation results, showing that the average errors in natural frequencies are less than 5 % and those in damping ratios are less than 10 %. The identified mode shapes are also compared with the exact values in Fig. 7, in which we observe good agreement with a minimum value of MAC [21] of 0.93. The first three mode shapes are modal behaviors with bounce, pitch, and roll modes, respectively, of the global motor vehicle, whereas the last four mode shapes are modal behaviors with bounce modes of the local left front, right front, left rear, and right rear wheels, respectively.

We also consider a linear 2D model of one-half of a railway vehicle excited by a simulated impulse loading. This simulated system in the numerical study, as shown in a sketch in Fig. 8, is identical to that in Ref. [19] and has the features of heavy damping (damping ratio above 10 %) and closely spaced modes (frequency separation smaller than 1.33 rad/sec). The system is a six-DOF system with $\mathbf{u} = [u_1, u_2, u_3, u_4, u_5, u_6]$, where $u_4 = \theta$ is the rotational displacement of the pitch behavior of the car body, and others are the vertical displacements of the bounce behavior of the car body, leading (trailing) bogies, and leading (trailing) wheelsets. The mass matrix is diagonal, diag $\mathbf{M}=[m_1, m_2, m_3, m_4, m_5, m_6]$, where $m_4 = I_B$ is the mass moment of inertia of the rigid body B at the top of the structure. The stiffness and damping matrices can be obtained as

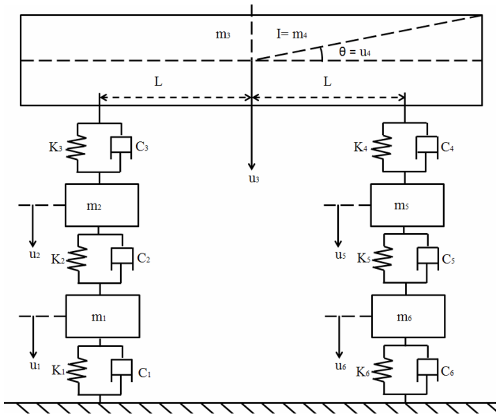

Fig. 8. Simplified 2D model of one-half railway vehicle.

$$\mathbf{K}=\begin{bmatrix} k_1+k_2 & -k_2 & 0 & 0 & 0 & 0 \\ -k_2 & k_2+k_3 & -k_3 & -k_3L & 0 & 0 \\ 0 & -k_3 & k_3+k_4 & k_3L-k_4L & -k_4 & 0 \\ 0 & -k_3L & k_3L-k_4L & k_3L^2+k_4L^2 & k_4L & 0 \\ 0 & 0 & -k_4 & k_4L & k_4+k_5 & -k_5 \\ 0 & 0 & 0 & 0 & -k_5 & k_5+k_6 \end{bmatrix},$$

$$\mathbf{C}=\begin{bmatrix} c_1+c_2 & -c_2 & 0 & 0 & 0 & 0 \\ -c_2 & c_2+c_3 & -c_3 & -c_3L & 0 & 0 \\ 0 & -c_3 & c_3+c_4 & c_3L-c_4L & -c_4 & 0 \\ 0 & -c_3L & c_3L-c_4L & c_3L^2+c_4L^2 & c_4L & 0 \\ 0 & 0 & -c_4 & c_4L & c_4+c_5 & -c_5 \\ 0 & 0 & 0 & 0 & -c_5 & c_5+c_6 \end{bmatrix},$$

where L is the horizontal distance between the center of the rigid body B and the springs/dashpots. Throughout this numerical study, $[m_1, m_2, m_3, m_5, m_6] = [1200, 850, 4125, 850, 1220]$ kg, and $m_4 = I_B = 1.25\times10^5\ \text{kg}\cdot\text{m}^2$; $k_1 = k_6 = 3.0\times10^7$ N/m, $k_2 = k_5 = 1.0\times10^6$ N/m, and $k_3 = k_4 = 6.0\times10^6$ N/m; $c_1 = c_6 = 0$, $c_2 = c_5 = 6.0\times10^3$ N·sec/m, and $c_3 = c_4 = 1.8\times10^4$ N·sec/m; $L = 8.53$ m. The damping matrix $\boldsymbol{C}$ that cannot be expressed as a linear combination of $\boldsymbol{M}$ and $\boldsymbol{K}$; thus, this one-half of a railway vehicle is a six-DOF non-proportionally damped system. The simulated impulse function serves as the excitation input acting on each mass point of the system. The sampling interval is set as $\Delta t = 0.01$ s, and

Table 4. Results of the modal estimation of a six-DOF system of a railway vehicle through the modified PolyMAX method with polynomial order $m = 4$.

Mode	Natural frequency (rad/s)			Damping ratio (%)			MAC
	Exact	PolyMAX	Error (%)	Exact	PolyMAX	Error (%)	
1	17.51	17.55	0.19	4.89	4.84	0.96	0.99
2	23.31	23.28	0.12	6.62	6.53	1.31	0.98
3	103.96	96.27	7.40	16.65	14.24	14.45	0.93
4	121.07	109.50	9.56	18.78	15.34	18.33	0.91
5	159.31	144.61	9.23	1.74	1.26	27.59	0.87
6	160.64	145.42	9.48	1.75	1.27	27.89	0.89

the sampling period is $T = N_t \cdot \Delta t = 81.92$ s.

Table 4 summarizes the modal-estimation results obtained from the simulated impulse response data, showing that the errors in natural frequencies and damping ratios are less than 10 % and 30 %, respectively. By solving a simplified generalized eigenvalue problem of the equation of motion in the state-space form of the six-DOF non-proportionally damped system, the "exact" modal damping ratios, as listed in Table 4, are the equivalent values obtained from the free-vibration analysis of the structural system with nonproportional damping. In addition, the result is in good agreement with the minimum value of MAC [21] between the identified and exact mode shapes of approximately 0.87. The modal analysis of numerical simulation models of a sedan and one-half of a railway vehicle is relatively complicated, but such analysis remains applicable for an accurate numerical simulation to confirm the validity of the proposed modal-estimation method.

To demonstrate the effectiveness of the present method for relatively practical structural systems with the experimental point of view, we considered an actual plate example. An experimental testing is conducted on a plate, which is tested under a free-free boundary condition and suspended by simple strings. A Brüel & Kjær RT Pro Photon 7.0 data acquisition system, along with PCB piezoelectric accelerometer 352B10 (with 10.3 mV/g sensitivity and 10 kHz frequency range), and a PCB impulse hammer 086C03 (with 2.25 mV/N sensitivity and 2224 N measurement range) are used to measure the response of the structure.

This experimental testing consisted of a 150 mm × 150 mm rectangular steel plate, which is studied in modal testing condition. The thickness of the plate is 3 mm. As the sides of the structure only slightly differ (0.25-5 mm), the plate will have closely spaced modes. To confirm this assumption, a simple finite element model of the plate is created, and the approximate natural frequencies and mode shapes of the structure are identified. This structure possesses at least one pair of closely spaced (even probably repeated) modes around 1160 Hz, as shown in Fig. 9 and Table 5. Currently, an FRF-based roving hammer testing is performed to measure the actual modal properties of the plate structure. Fig. 10 shows the experiment setup of this test. Sixteen points on the plate are marked and

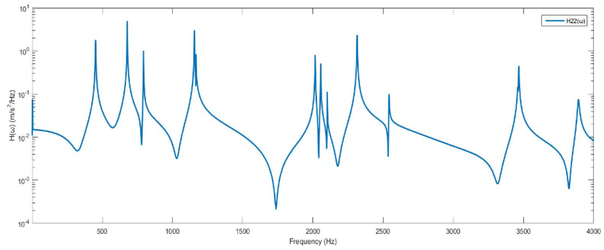

Fig. 9. Typical plot of the amplitude frequency response function $H_{22}(\omega)$ of the system showing at least a pair of closely spaced (even repeated) modes around 1160 Hz.

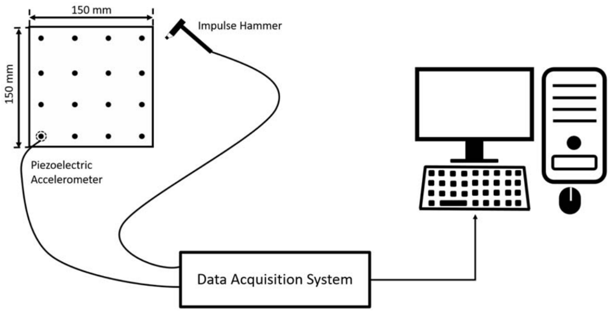

Fig. 10. Schematics of experiment setup of hammer testing for actual plate.

hammer impacts are acted through these 16 locations of the plate. For the EMA testing, a simple hammer, to which the force sensor is attached, is used to excite the structure with a steel tip.

Through this simple hammer testing, the 256 acceleration responses are extracted by a sampling frequency of 12800 Hz and recording length of approximately 0.5 s. Then, a stabilization diagram with different model orders can be constructed using the PolyMAX method, as shown in Fig. 11. The natural frequencies and damping ratios of the plate are estimated directly by solving the eigenvalue problem associated with the companion matrix constructed by denominator polynomial coefficients, as listed in Table 5. The "exact" modal frequencies and damping ratios listed in Table 5, as well as the exact mode shapes, are the equivalent values obtained by using the ibrahim time-domain (ITD) method from the impulse acceleration response data of the practical plate structure. These results show that the accuracy of the modified PolyMAX method in calculating the natural frequencies of closely spaced modes of the plate is reasonable. In general, as the structural response is less sensitive to damping ratios than to the natural frequencies, the identification errors of damping ratios, as shown in Table 5, are relatively higher, but the accuracy is acceptable.

Table 5 lists the results of MAC verification between the mode shapes identified by the modified PolyMAX method and by modal testing. In Table 5, the mode shapes of the closely spaced modes are reasonably consistent with those extracted by hammer testing. The MAC values for the mode

Table 5. Results of the modal estimation of a practical plate through the modified PolyMAX method with polynomial order $m = 100$.

Mode	Natural frequency (Hz)			Damping ratio (%)			MAC
	ITD	PolyMAX	Error (%)	ITD	PolyMAX	Error (%)	
1	452.81	451.43	0.30	2.18	2.48	13.76	0.99
2	678.57	674.97	0.53	1.01	1.07	5.94	0.98
3	794.47	797.88	0.43	0.99	0.84	15.15	1.00
4	1156.76	1159.23	0.21	0.93	0.81	12.90	1.00
5	1167.37	1161.39	0.51	0.52	0.58	11.54	0.97
6	2015.91	2020.57	0.23	0.44	0.61	38.64	0.98
7	2055.59	2072.68	0.83	0.24	0.33	37.50	1.00
8	2315.27	2329.52	0.62	0.81	0.86	6.17	0.76
9	2542.59	2535.75	0.27	0.29	0.18	37.93	0.89
10	3466.09	3454.02	0.35	0.37	0.41	10.81	1.00
11	3889.63	3900.03	0.27	2.18	2.48	13.76	0.99

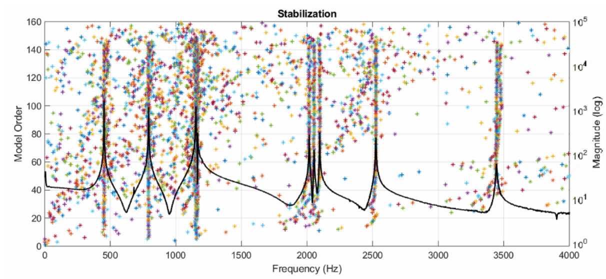

Fig. 11. Typical plot of the stabilization diagram and $H_{11}(\omega)$ of the actual plate with a pair of closely spaced modes.

shapes estimated by the ITD and modified PolyMAX methods show that each set of mode shapes is well correlated within itself. Therefore, both methods present great robustness in identifying well-correlated mode shapes for the plate.

In this study, the multi-reference identification of the PolyMAX method is used to implement the parametric estimation of structures with modal interference. In the procedure of modal estimation, we propose a modification to replace the rational fraction in the form of conventional scalar coefficients by constructing the frequency response function matrix of the rational fraction of the matrix coefficients. We can thus prevent the incomplete modal information obtained from the scalar-coefficient rational fraction from the single-frequency response function only. A high polynomial order for the PolyMAX method can be significantly reduced when the rational fraction of the matrix coefficients is used, and further accuracy of modal estimation can be effectively performed. In addition, such approach may significantly improve the computation efficiency in that modal identification can be implemented by solving the eigenproblem of the companion matrix only. The proposed algorithm is applicable for improving the validity and accuracy of the modal estimation of the system with modal interference.

5. Conclusions

The extent of interference among structural modes may often affect the accuracy of parametric estimation during modal identification. In this paper, the matrix-fractional coefficient model constructed by MDOF frequency response functions in the modified PolyMAX method is presented to perform the system identification of structures with modal interference. By introducing a system model with higher-order matrix-fractional coefficients in conjunction with the different-order constructed stabilization diagram during modal estimation, we can determine the number of modes to be identified. We can thus avoid the erroneous estimation of the modal frequencies to be identified for the case of an MDOF system with modal interference only upon the phase angle diagram of the frequency response function. Furthermore, the modal parameters of systems can be obtained by solving the eigenproblem of the companion matrix yielded from least-square estimation. Moreover, the computation required for the conventional PolyMAX method can be significantly reduced. Numerical simulations, including a full model of sedan and one-half railway vehicle in the form of a linear 2D model, as well as the experimental testing of an actual plate, confirm the validity and robustness of the proposed parametric-estimation method for a system with modal interference under noisy conditions.

Acknowledgments

This research was supported in part by the Ministry of Science and Technology of Taiwan under the Grant MOST 107-2221-E-020-010-. The author wishes to thank anonymous reviewers for their valuable comments and suggestions in revising the paper.

Nomenclature

$[H(\omega)]$: Frequency response function matrix
$[A(\omega)]$: Common denominator polynomial matrix
$[B(\omega)]$: Numerator polynomial matrix
$\otimes$: Kronecker product
$\boldsymbol{M}$: Mass matrix
$\boldsymbol{K}$: Stiffness matrix
$\boldsymbol{C}$: Damping matrix
m : Polynomial order

References

[1] S. A. H. Kordkheili, S. H. M. Massouleh, M. J. Kokabi and H. Bahai, A modal coupling procedure to improve residual modal effects based on experimentally generated data, *Journal of Sound and Vibration*, 331 (1) (2012) 66-80.

[2] S. A. H. Kordkheili, S. H. M. Massouleh, S. Hajirezayi and H. Bahai, Experimental identification of closely spaced modes using NExT-ERA, *Journal of Sound and Vibration*,

412 (6) (2018) 116-129.
[3] J. O. Hougen and R. A. Walsh, Pulse testing method, *Chemical Engineering Progress*, 57 (3) (1961) 69-79.
[4] E. O. Brigham, *The Fast Fourier Transform,* Prentice-Hall (1974).
[5] F. R. Spitznogle and A. H. Quazi, Representation and analysis of time-limited signal using a complex exponential algorithm, *Journal of the Acoustical Society of America*, 47 (5) (1970) 1150-1155.
[6] W. R. Smith, Least squares time-domain methods for simultaneous identification of vibration parameters from multiple free-response records, *AIAA/ASME/ASCE/AHS 22nd SDM Conference,* April (1981) 194-201.
[7] H. Vold, J. Kundrat, G. T. Rocklin and R. Russell, A multi-input modal estimation algorithm for mini-computers, *SAE Technical Paper Series*, 91 (1) (1982) 815-821.
[8] M. H. Richardson and D. L. Formenti, Parameter estimation from frequency response measurements using rational fraction polynomials, *Proceedings of the 1st International Modal Analysis Conference*, Orlando, Florida, November 8-10 (1982).
[9] H. Van der Auweraer, P. Guillaume, P. Verboven and S. Vanlanduit, Application of a fast-stabilizing frequency domain parameter estimation method, *Journal of Dynamic Systems Measurement and Control - Transactions of the ASME* (2001) 651-658.
[10] P. Guillaume, P. Verboven, S. Vanlanduit, H. Van Der Auweraer and B. Peeters, A poly-reference implementation of the least-squares complex frequency-domain estimator, *International Modal Analysis Conference (IMAC XXI)*, Kissimmee, Florida (2003).
[11] H. Van der Auweraer and B. Peeters, Discriminating physical poles from mathematical poles in high order systems: Use and automation of the stabilization diagram, *Proceedings of the IEEE Instrumentation and Measurement Technology Conference*, Como, Italy, May (2004) 2193-2198.
[12] B. Peeters, H. Van der Auweraer and P. Guillaume, The PolyMAX frequency-domain method: A new standard for modal parameter estimation, *Shock and Vibration*, 11 (3-4) (2004) 395-409.
[13] X. Liu, Y. Luo, B. W. Karney, Z. Wang and L. Zhai, Virtual testing for modal and damping ratio identification of submerged structures using the PolyMAX algorithm with two-way fluid-structure interactions, *Journal of Fluids and Structures*, 54 (2015) 548-565.
[14] P. Sitarz and B. Powalka, Modal parameters estimation using colony optimization algorithm, *Mechanical Systems and Signal Processing*, 76-77 (2016) 531-554.
[15] T. D. Troyer, P. Guillaume and G. D. Sitter, Improved poly-reference frequency-domain modal estimators for flutter analysis, *14th IFAC Symposium on System Identification,* Newcastle, Australia (2006).
[16] R. Shirzadeh, C. Devriendt, M. A. Bidakhvidi and P. Guillaume, Experimental and computational damping estimation of an offshore wind turbine on a monopile foundation, *Journal of Wind Engineering and Industrial Aerodynamics*, 120 (2013) 96-106.
[17] C. Geng, F. Wang, J. Zhang and Z. Jin, Modal parameters identification of power transformer winding based on improved empirical mode decomposition method, *Electric Power Systems Research*, 108 (2014) 331-339.
[18] W. J. Yi, Y. Zhou, S. Kunnath and B. Xu, Identification of localized frame parameters using higher natural modes, *Engineering Structures*, 30 (2008) 3082-3094.
[19] C.-S. Lin, Parametric estimation of systems with modal interference, *Archive of Applied Mechanics*, 87 (2017) 1845-1857.
[20] N. M. Newmark, A method of computation for structural dynamics, *ASCE Journal of Engineering Mechanics Division*, 85 (1959) 67-74.
[21] R. L. Allemang and D. L. Brown, A correlation coefficient for modal vector analysis, *Proceedings of the 1st International Modal Analysis Conference,* Society for Experiment Mechanics, Bethel, CT (1983) 110-116.
[22] S. S. Rao, Coordinate coupling and principal coordinates, *Mechanical Vibrations*, 5th Ed., Person, United States (2011) 488-491.

C. S. Lin received his Ph.D. from the Department of Aeronautics and Astronautics of National Cheng Kung University, Taiwan, in 2011. He joined the Faculty of National Pingtung University of Science and Technology, Taiwan, in 2016 where he is currently an Assistant Professor at the Department of Vehicle Engineering. His research interests are random vibration and modal analysis.